Crystal structure of 3-[(3,4-dinitro-1*H*-pyrazol-1-yl)-*NNO*-azoxy]-4-nitro-1,2,5-oxadiazole

A. O. Dmitrienko [1,a)] A. A. Konnov,[2] and M. S. Klenov[2]
[1]*Department of Chemistry, M. V. Lomonosov Moscow State University, 1 Leninskie Gory, Moscow 119991, Russian Federation*
[2]*N. D. Zelinsky Institute of Organic Chemistry, Russian Academy of Sciences, 47 Leninsky Prosp., Moscow 119991, Russian Federation*

(Received 3 September 2020; accepted 16 March 2021)

The crystal structure of a novel high-energy density material 3-[(3,4-dinitro-1*H*-pyrazol-1-yl)-*NNO*-azoxy]-4-nitro-1,2,5-oxadiazole $C_5HN_9O_8$ was determined and refined using laboratory powder diffraction data. The diffraction data and database analysis were insufficient to distinguish two candidate structures from the solution step. Density functional theory with periodic boundary conditions optimizations were used to choose the correct one. 3-[(3,4-Dinitro1*H*-pyrazol-1-yl)-*NNO*-azoxy]-4-nitro-1,2,5-oxadiazole crystallizes in space group *Pbca* with $a = 8.3104(2)$ Å, $b = 14.2198(5)$ Å, $c = 19.4264(7)$ Å, $V = 2295.66(14)$ Å^3. The molecular conformation contains a weak intramolecular hydrogen bond C–H···O–N, and the structure is dominated by weak O···π and O···O contacts.
 [doi:10.1017/S0885715621000233]

Key words: Rietveld refinement, DFT calculations, high-energy density materials

I. INTRODUCTION

X-ray powder diffraction techniques are routinely used in the analysis of high-energy density materials (HEDMs). Their main objectives are phase analysis and calculation of crystal density at room temperature. When single-crystal experiments are unavailable, they are also used to determine the crystal structure (and thus confirm the molecular structure) (Klenov *et al.*, 2016).

High-energy density materials containing the azoxy group are a subject of intensive research (Fischer *et al.*, 2014; Yu *et al.*, 2015; Liu *et al.*, 2016). However, only few (and not high-energy) compounds with an azoxy group bonded to a nitrogen atom of the heterocycle were reported (Moriarty *et al.*, 1990; Semenov *et al.*, 1992). Additional N–N bond can increase the enthalpy of formation and thus energy density. A molecular diagram for 3-[(3,4-dinitro-1*H*-pyrazol-1-yl)-*NNO*-azoxy]-4-nitro-1,2,5-oxadiazole $C_5HN_9O_8$ is shown in Figure 1.

II. EXPERIMENTAL

A. Safety precautions

Although we have encountered no difficulties during the preparation and handling of compound described in this paper, it is a potentially explosive energetic material that is sensitive to impact and friction. Mechanical actions of this energetic material, involving scratching or scraping, must be avoided. Any manipulations must be carried out by using appropriate standard safety precautions (face shield, ear protection, body armor, Kevlar® gloves, and grounded equipment).

3-[(3,4-Dinitro-1*H*-pyrazol-1-yl)-*NNO*-azoxy]-4-nitro-1,2,5-oxadiazole was synthesized in three steps from known 1-amino-3,4-dinitropyrazole (Yin *et al.*, 2014) as part of Russian Science Foundation project 19-13-00276.

The compound is an impact and friction-sensitive explosive, so caution is needed during sample preparation. The sample was ground in an agate mortar in small (~5 mg) portions and placed between two Kapton films with a PTFE spatula.

The powder pattern was measured on a Bruker AXS D8 Advance Vario powder diffractometer equipped with primary monochromator (Cu$K\alpha_1$, $\lambda = 1.54056$ Å) and 1D LynxEye PSD. Data were collected at room temperature in the range 2–60° in 2θ with a 0.01° 2θ step size and 1 s step^{-1} in transmission mode (Figure 2).

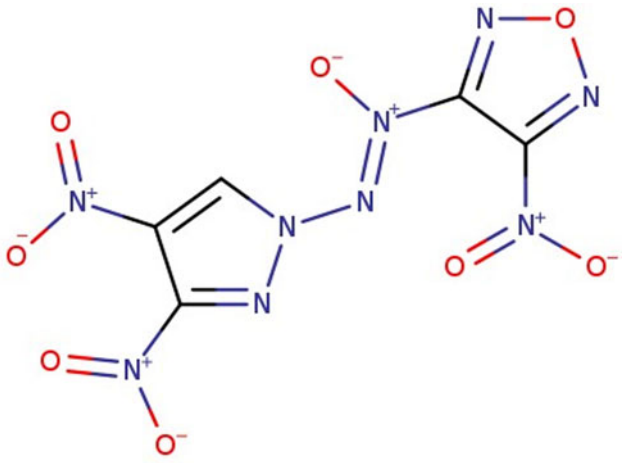

Figure 1. The molecular structure of 3-[(3,4-dinitro-1*H*-pyrazol-1-yl)-*NNO*-azoxy]-4-nitro-1,2,5-oxadiazole.

[a)]Author to whom correspondence should be addressed. Electronic mail: dmitrienka@gmail.com

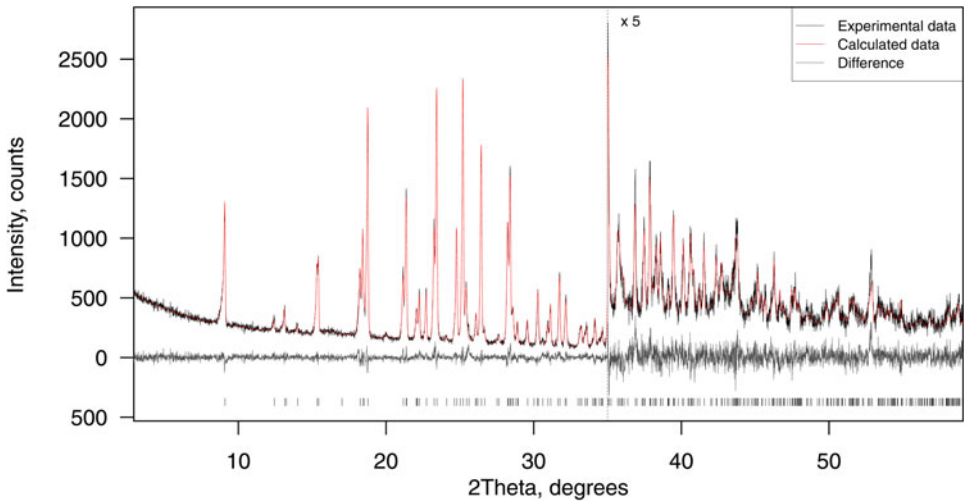

Figure 2. Final observed (black), calculated (red), and difference profiles for the Rietveld refinement.

The diffraction pattern was indexed on a primitive orthorhombic cell with $a = 8.3104(2)$ Å, $b = 14.2198(5)$ Å, $c = 19.4264(7)$ Å using the SVD (singular value decomposition) index algorithm (Coelho, 2003) as implemented in Bruker TOPAS 5.0 (Coelho, 2018), and space group determination was carried out using statistical systematic absences analysis as implemented in ExtSym (Markvardsen *et al.*, 2008). The resulting most probable space group *Pbca* was later confirmed by structure solution and refinement.

Parallel tempering, as implemented in FOX (Favre-Nicolin and Černý, 2002) was used to solve the crystal structure in direct space. The Rietveld refinement (with Bruker TOPAS 5.0) was carried out using bond and angle restraints derived from PW-DFT-D calculations and a "riding" model for the hydrogen atom. The restraint weight was automatically decreased during the refinement, and the refinement result of a more restrained model served as a starting structure for the next less restrained one. For a detailed explanation of the methodology, see Dmitrienko and Bushmarinov (2015).

PW-DFT-D calculations were performed in VASP5.4.4 (Kresse and Hafner, 1993, 1994; Kresse and Furthmüller, 1996a, 1996b) using the PBE functional (Perdew *et al.*, 1996) corrected by the Grimme D3 van der Waals correction (Grimme *et al.*, 2010) with Becke–Jonson damping (Grimme *et al.*, 2011). A plane-wave basis set with "normal" projector augmented wave (PAW) pseudopotentials (Blöchl, 1994; Kresse and Joubert, 1999) as supplied with VASP was employed. All optimizations were performed using an energy cutoff of 600 eV. Default 0.5 $Å^{-1}$ *k*-point mesh and 2 *k*-points were used in all calculations.

Root-mean-square (rms) Cartesian displacement between the Rietveld-refined structure and the PW-DFT-D-optimized ones were calculated as suggested by Neumann (van de Streek and Neumann, 2014).

III. RESULTS AND DISCUSSION

Parallel tempering runs in FOX lead to two global minimization solutions with almost identical χ^2; their views in crystals are shown in Figures 3 and 4. The only difference between the structures is the mutual arrangement of C–H and N-lone pair fragments of the pyrazole ring.

Both C–H and N-lone pair fragments contain seven electrons and it can be difficult to distinguish them even for a

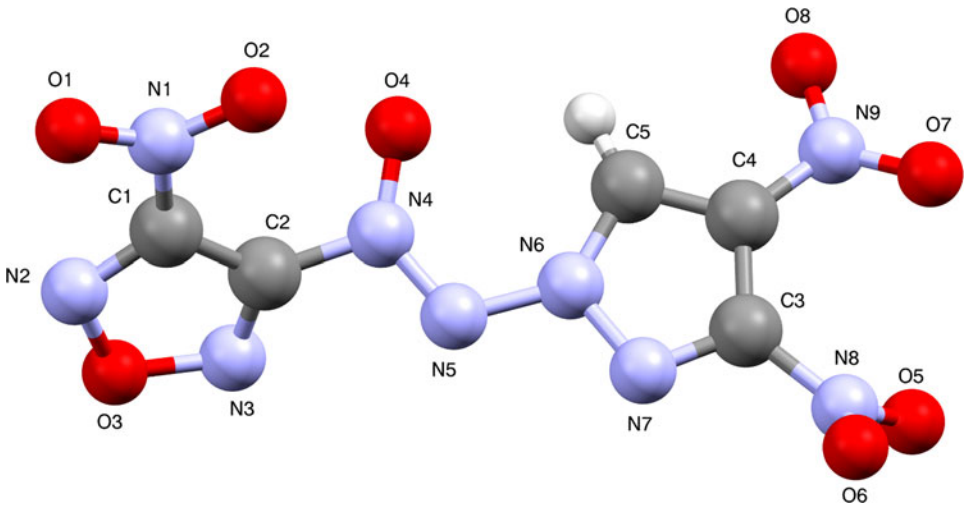

Figure 3. General view of **1** in a crystal.

https://doi.org/10.1017/S0885715621000233 Published online by Cambridge University Press

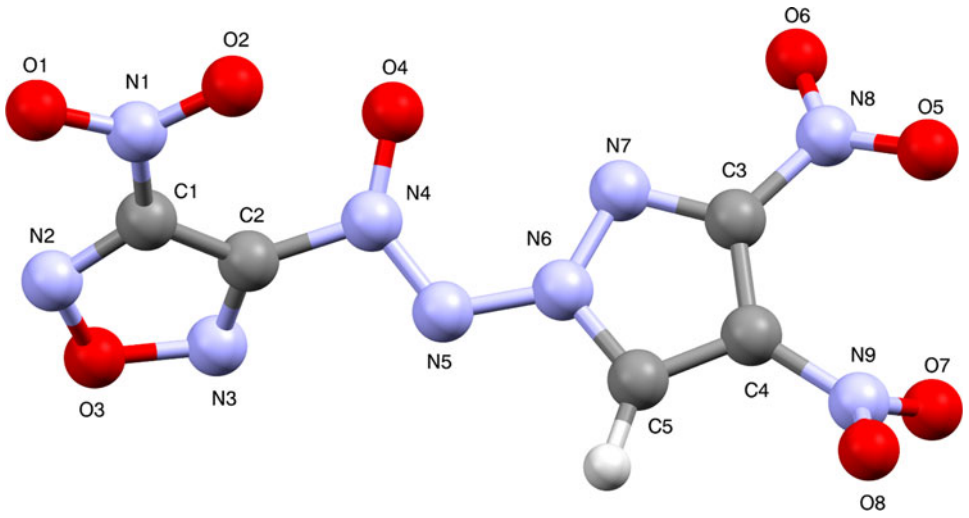

Figure 4. General view of **2** in a crystal.

medium quality single-crystal experiment. For Rietveld refinement where both atomic thermal parameters and Fourier maps are noisy, there is no way to do it reliably. In most cases, such ambiguity can be resolved by examining intermolecular contacts. But high-energy density material structures often lack strong hydrogen or halogen intermolecular bonds and contain only weak O···O and O···π contacts (Fedyanin *et al.*, 2019). Structures **1** and **2** share most contacts, the only differences are weak intramolecular C–H···O hydrogen bond with formation of 6-member cycle in **1** and weak intermolecular C–H···π interaction in **2**. No unusual contacts were found in either structure; it is not immediately obvious which structure is correct.

Another way to choose the correct solution is to optimize both structures with an appropriate quantum chemistry method and examine resulting energies and geometries. If one of the structures has much higher energy or the atomic coordinates vary significantly from experimental ones, we should dismiss that solution (van de Streek and Neumann, 2010). If energies and atomic positions are close, we should consider a statically disordered structure.

For structure **1,** PW-DFT-D-optimized energies are −1297.188/−1297.284 eV for fixed/relaxed cell calculations. For structure **2,** optimized energies are −1294.912/−1295.495 eV. So, structure **1** is more than 5 kcal mol^{-1} more energetically favorable. The difference is large: considering Boltzmann distribution at room temperature coexisting of two forms is improbable. Thus, we should dismiss structure **2** and accept structure **1**.

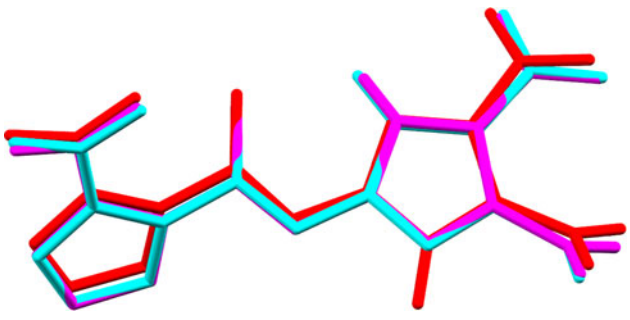

Figure 5. Comparison of energy-optimized structures **1** (cyan), **2** (red), and Rietveld-refined **1** (magenta).

After the solution step, the difference between **1** and **2** was merely a swap of C–H and N fragments in the pyrazole ring or, equivalently, 180° change in the C2–N4–N5–N6 torsion angle. Now, it is possible to discuss more subtle geometric features of the calculated structures; all the values discussed are related to the free-cell calculations. The most considerable differences are in the bond angle C5–N6–N5 (134.1° for **1** and 118.1° for **2**), the torsion angle C2–N4–N5–N6 (173.2° for **1** and 171.7° for **2**), and the dihedral angle between planes containing pyrazole and furazan rings (68.7° for **1** and 62.8° for **2**). The differences are associated with the intramolecular hydrogen bond in structure **1**.

Rietveld refinement was performed with fixed-cell energy-optimized structure **1** as source of bond and angle restraints. Final refinement with 98 variables and 56 restraints over 5536 data points yielded $R_p/R_p'/R_{wp}/R_{wp}'/R_{Bragg}$ = 6.08/16.96/8.41/17.47/2.31%, GOF = 1.26. The resulting Rietveld plot is shown in Figure 2. The rms Cartesian displacement between free-cell energy-optimized structure **1** and final Rietveld-refined structure is 0.083, which is within the range expected for correct structures. Comparison of the final Rietveld-refined structure with fixed-cell energy-minimized structures **1** and **2** is shown in Figure 5.

Figure 6 depicts the packing of **1**. The shortest intermolecular contact in the structure is the O···π interaction between the nitro group and the furozan cycle with the O···C distance 2.851 Å. Other notable contacts are NO_2···O_2N (O···O distance is 2.938 Å), NO_2···N(O)N (O···N distance is 2.930 Å), and another NO_2···π (O···C distance is 2.937 Å). A lack of strong intermolecular interactions is typical for HEDMs.

IV. DEPOSITED DATA

The Crystallographic Information File (ak170.cif) that contains the results of the Rietveld refinement and the raw powder diffraction pattern, and four files (VASP_1_refined_cell.cif, VASP_1_fixed_cell.cif, VASP_2_refined_cell.cif, VASP_2_fixed_cell.cif) related to the PW-DFT-D calculations using VASP were deposited with ICDD. The VASP

https://doi.org/10.1017/S0885715621000233 Published online by Cambridge University Press

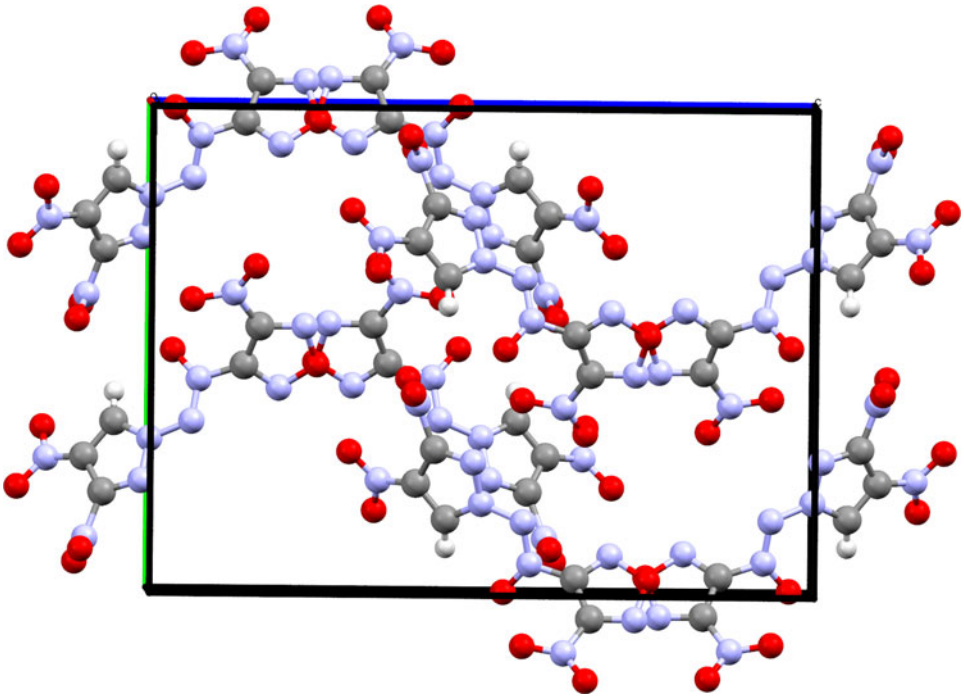

Figure 6. Fragment of the crystal packing of **1** (view along the *a*-axis).

files were used to obtain the bond length and angle restraints and for geometry discussion. These data files can be requested at info@icdd.com. The first file is also available from CCDC 2025381.

ACKNOWLEDGEMENTS

The study was funded by RFBR according to the research project № 1933-60075. M. S. Klenov and A. A. Konnov acknowledge financial support from the Russian Science Foundation (project 19-13-00276) for the synthesis of the title compound. The *in crystal* calculations were carried out using the equipment of the shared research facilities of HPC computing resources at Lomonosov Moscow State University (Sadovnichy et al., 2013).

Blöchl, P. E. (**1994**). "Projector augmented-wave method," Phys. Rev. B **50** (24), 17953–17979.

Coelho, A. A. (**2003**). "Indexing of powder diffraction patterns by iterative use of singular value decomposition," J. Appl. Crystallogr. **36**(1), 86–95.

Coelho, A. A. (**2018**). "TOPAS and TOPAS-academic: an optimization program integrating computer algebra and crystallographic objects written in C++," J. Appl. Crystallogr. **51**(1), 210–218.

Dmitrienko, A. O. and Bushmarinov, I. S. (**2015**). "Reliable structural data from Rietveld refinements via restraint consistency," J. Appl. Crystallogr. **48**(6), 1777–1784.

Favre-Nicolin, V. and Černý, R. (**2002**). "FOX, "free objects for crystallography": a modular approach to *ab initio* structure determination from powder diffraction," J. Appl. Crystallogr. **35**(6), 734–743.

Fedyanin, I. V., Lyssenko, K. A., Fershtat, L. L., Muravyev, N. V., and Makhova, N. N. (**2019**). "Crystal solvates of energetic 2,4,6,8,10,12-hexanitro-2,4,6,8,10,12-hexaazaisowurtzitane molecule with [bmim]-based ionic liquids," Cryst. Growth Des. **19**(7), 3660–3669.

Fischer, D., Klapötke, T. M., Reymann, M., and Stierstorfer, J. (**2014**). "Dense energetic nitraminofurazanes," Chemistry **20**(21), 6401–6411.

Grimme, S., Antony, J., Ehrlich, S., and Krieg, H. (**2010**). "A consistent and accurate ab initio parametrization of density functional dispersion correction (DFT-d) for the 94 elements H-Pu," J. Chem. Phys. **132**(15), 154104.

Grimme, S., Ehrlich, S., and Goerigk, L. (**2011**). "Effect of the damping function in dispersion corrected density functional theory," J. Comput. Chem. **32**(7), 1456–1465.

Klenov, M. S., Anikin, O. V., Guskov, A. A., Churakov, A. M., Strelenko, Y. A., Ananyev, I. V., Bushmarinov, I. S., Dmitrienko, A. O., Lyssenko, K. A., and Tartakovsky, V. A. (**2016**). "Serendipitous synthesis of (tert-butyl-*NNO*-azoxy)acetonitrile: reduction of an oxime moiety to a methylene unit," Eur. J. Org. Chem. **2016**(22), 3845–3855.

Kresse, G. and Furthmüller, J. (**1996a**). "Efficiency of ab-initio total energy calculations for metals and semiconductors using a plane-wave basis set," Comput. Mater. Sci. **6**(1), 15–50.

Kresse, G. and Furthmüller, J. (**1996b**). "Efficient iterative schemes for *ab initio* total energy calculations using a plane-wave basis set," Phys. Rev. B **54**(16), 11169–11186.

Kresse G., and Hafner, J. (**1993**). "*Ab initio* molecular dynamics for liquid metals," Phys. Rev. B **47**(1), 558–561.

Kresse, G., and Hafner, J. (**1994**). "*Ab initio* molecular-dynamics simulation of the liquid-metal–amorphous-semiconductor transition in germanium," Phys. Rev. B **49**(20), 14251–14269.

Kresse, G. and Joubert, D. (**1999**). "From ultrasoft pseudopotentials to the projector augmented-wave method," Phys. Rev. B **59**(3), 1758–1775.

Liu, Y., Zhang, J., Wang, K., Li, J., Zhang, Q., and Shreeve, J. (**2016**). "Bis (4-nitraminofurazanyl-3-azoxy)azofurazan and derivatives: 1,2,5-oxadiazole structures and high-performance energetic materials," Angew. Chem., Int. Ed. **55**(38), 11548–11551.

Markvardsen, A. J., Shankland, K., David, W. I. F., Johnston, J. C., Ibberson, R. M., Tucker, M., Nowell, H., and Griffin, T. (**2008**). "Extsym: a program to aid space-group determination from powder diffraction data," J. Appl. Crystallogr. **41**(6), 1177–1181.

Moriarty, R. M., Hopkins, T. E., Prakash, I., Vaid, B. K., and Vaid, R. K. (**1990**). "Hypervalent iodine oxidation of amines in the presence of nitroso compounds: a method for the preparation of unsymmetrically substituted azoxy compounds," Synth. Commun. **20**(15), 2353–2357.

Perdew, J. P., Burke, K., and Ernzerhof, M. (**1996**). "Generalized gradient approximation made simple," Phys. Rev. Lett. **77**(18), 3865–3868.

Sadovnichy, V., Tikhonravov, A., Voevodin, V., and Opanasenko, V. (**2013**). "'Lomonosov': Supercomputing at Moscow State University," in

Contemporary High Performance Computing: From Petascale toward Exascale, edited by Jeffrey S. Vetter (Chapman and Hall/CRC Computational Science, Boca Raton, USA), pp. 283–307.

Semenov, S. E., Churakov, A. M., Chertanova, L. F., Strelenko, Y. A., Ioffe, S. L., and Tartakovskii, V. A. (**1992**). "Synthesis of 1-(2,4,6-trichlorophenyl)2-(1,2,4-triazol-4-yl)-diazene-1-oxide," Bull. Russ. Acad. Sci. Div. Chem. Sci. **41**(2), 277–279.

van de Streek, J. and Neumann, M. A. (**2010**). "Validation of experimental molecular crystal structures with dispersion-corrected density functional theory calculations," Acta Crystallogr. Sect. B Struct. Sci. **66**(5), 544–558.

van de Streek, J. and Neumann, M. A. (**2014**). "Validation of molecular crystal structures from powder diffraction data with dispersion-corrected density functional theory (DFT-d)," Acta Crystallogr. Sect. B Struct. Sci., Cryst. Eng. Mater. **70**(6), 1020–1032.

Yin, P., Zhang, J., He, C., Parrish, D. A., and Shreeve, J. M. (**2014**). "Polynitro-substituted pyrazoles and triazoles as potential energetic materials and oxidizers," J. Mater. Chem. A **2**, 3200–3208.

Yu, Q., Wang, Z., Yang, H., Wu, B., Lin, Q., Ju, X., Lu, C., and Cheng, G. (**2015**). "N-trinitroethyl-substituted azoxyfurazan: high detonation performance energetic materials," RSC Adv. **5**(35), 27305–27312.

https://doi.org/10.1017/S0885715621000233 Published online by Cambridge University Press